Human Kinetic Modeling of the 5HT6 PET Radioligand ^{11}C-GSK215083 and Its Utility for Determining Occupancy at Both 5HT6 and 5HT2A Receptors by SB742457 as a Potential Therapeutic Mechanism of Action in Alzheimer Disease

Christine A. Parker[1,2], Eugenii A. Rabiner[3,4], Roger N. Gunn[2,3,5], Graham Searle[2], Laurent Martarello[6], Robert A. Comley[7], Maria Davy[8], Alan A. Wilson[9], Sylvain Houle[9], Romina Mizrahi[9], Marc Laruelle[10], and Vincent J. Cunningham[11]

[1]GlaxoSmithKline, Clinical Imaging Centre, Hammersmith Hospital, London, United Kingdom; [2]Division of Brain Sciences, Department of Medicine, Imperial College London, London, United Kingdom; [3]Imanova Ltd., Imperial College London, London, United Kingdom; [4]Centre for Neuroimaging Sciences, Institute of Psychiatry, Psychology and Neuroscience, King's College, London, United Kingdom; [5]Department of Engineering Science, University of Oxford, Oxford, United Kingdom; [6]AbbVie, Translational Imaging, Integrated Science and Technology, North Chicago, Illinois; [7]Roche Pharmaceutical Research and Early Development, Basel, Switzerland; [8]GlaxoSmithKline, Neuroscience Therapy Area Unit, Stevenage, United Kingdom; [9]Research Imaging Centre, CAMH, and Department of Psychiatry, University of Toronto, Toronto, Canada; [10]Intra-Cellular Therapies Inc., New York, New York; and [11]School of Medical Sciences, University of Aberdeen, Aberdeen, United Kingdom

Antagonism of 5-hydroxytrypamine-6 (5HT6) receptors is associated with procognitive effects in preclinical species, suggesting a therapeutic potential for this mechanism in Alzheimer disease (AD) and other cognitive diseases. In a phase 2 dose study, SB742457, a novel 5HT6 antagonist, showed increasing procognitive effects in patients with AD as the dose increased, with a procognitive signal in AD patients at a dose of 35 mg/d superior to the other doses tested (5 and 15 mg/d). **Methods:** In this article, we describe the quantification and pharmacologic selectivity of a new 5HT6 PET ligand (^{11}C-GSK215083) in healthy volunteers and its use to measure occupancies achieved at various doses of SB742457. **Results:** Kinetic analysis of ^{11}C-GSK215083 uptake in the human brain demonstrated the multilinear model, MA2, to represent the method of choice when a blood input was available and the full tissue reference method when no input was available. Pharmacologic dissection of the in vivo ^{11}C-GSK215083–specific binding showed the ligand bound mostly the 5HT6 in the striatum (blocked by SB742457 but not by the selective 5-hydroxytryptamine-2A (5HT2A) antagonist ketanserin) and the 5HT2A in the frontal cortex (blocked by both ketanserin and SB742457). Repeated administration of SB742457 (3, 15, and 35 mg/d) saturated the 5HT6 receptors at all doses. In the cortex, 5HT2A receptor occupancy was 24% ± 6% (3 mg/d), 35% ± 4% (15 mg/d), and 58% ± 19% (35 mg/d; mean ± SD), suggesting a progressive engagement of 5HT2A as the dose increased. **Conclusion:** Collectively, these data support the use of ^{11}C-GSK215083 as a 5HT6 clinical imaging tool and suggest that blocking both the 5HT6 and the 5HT2A receptors may be required for the optimal therapeutic action of SB742457 in AD.

Received Jun. 25, 2015; revision accepted Aug. 28, 2015.
For correspondence or reprints contact: Christine Parker, GlaxoSmithKline, Medicines Research Centre, Gunnels Wood Rd., Stevenage, Hertfordshire, SG1 2NY, U.K.
E-mail: Christine.A.Parker@gsk.com
Published online Sep. 17, 2015.

Key Words: 5HT6; human kinetic modeling; ^{11}C-GSK215083; SB742457; Alzheimer's disease

J Nucl Med 2015; 56:1901–1909
DOI: 10.2967/jnumed.115.162743

The 5-hydroxytrypamine-6 (5HT6) receptor is a 7-transmembrane receptor expressed in the mammalian central nervous system, through which serotonin acts to regulate several biologic processes (*1*). Both in vitro and in vivo imaging studies have demonstrated high levels of this receptor in the basal ganglia and limbic structures of the brain, moderate levels in the cortical structures, and low levels in the cerebellar regions (*2,3*). Preclinical studies have demonstrated cognitive-enhancing effects of 5HT6 antagonism (*4*), prompting the development of 5HT6 antagonists for the symptomatic treatment of cognitive disorders such as Alzheimer disease (AD).

SB742457 is a novel 5HT6 receptor antagonist under development for cognitive remediation in AD (*5–7*). In a phase 2 dose-ranging study (*5*), 3 dose levels were investigated (5, 15, and 35 mg once daily for 24 wk) in a randomized, double-blind, placebo-controlled study in 357 subjects with mild-to-moderate probable AD. The highest dose level separated from placebo on the Clinician's Interview-Based Impression of Change with caregiver input (CIBIC+) score, whereas the lower doses did not. These data suggest the usefulness of 5HT6 antagonism in the symptomatic treatment of AD.

Occupancies of the 5HT6 receptor achieved in these clinical studies have not yet been conveyed. We previously reported the development, radiosynthesis, preclinical assessment, and initial human evaluation of the selective, high-affinity 5HT6 receptor PET ligand ^{11}C-GSK215083 (*3,8*). Collectively, these data suggest ^{11}C-GSK215083 would be a useful tracer to label 5HT6 receptors in the human brain.

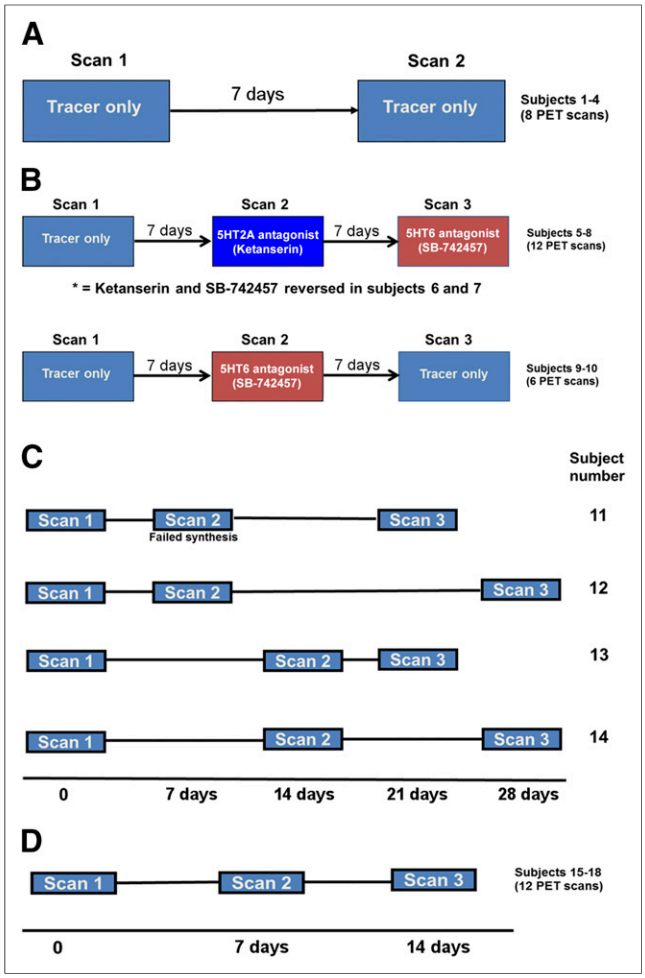

FIGURE 1. Study design. Subjects were divided into 3 groups. (A) Test–retest (n = 4). (B) Pharmacologic characterization of ^{11}C-GSK215083 for 5HT6 receptor in striata using SB742457 and 5HT2A receptor in the cortex using ketanserin (n = 6). (C and D) Time and dose occupancy of SB742457 (n = 8) where scan 1 = baseline scan and scans 2 and 3 following repeated once daily dosing of SB742457 at 2 time intervals between 7 and 28 d of dosing.

In this study, we report first the kinetic methods to derive ^{11}C-GSK215083 binding potential (BP) in the human brain; second, investigation of ^{11}C-GSK215083 selectivity for both the 5HT6 and the 5-hydroxytryptamine-2A (5HT2A) receptors (as this radioligand displayed only ~5-fold difference in selectivity for the 5HT6 versus 5HT2A (*3*)); and third, evaluation of 5HT6 and 5HT2A receptor occupancy achieved upon repeated administration of various doses of SB742457.

MATERIALS AND METHODS

Radiosynthesis of ^{11}C-GSK215083

GSK215083 and the *N*-desmethyl precursor were prepared according to published procedures (*9,10*). All other chemicals and solvents were of analytic grade.

PET studies were performed at 2 facilities: the Centre for Addiction and Mental Health (CAMH) in Toronto, Canada, and the Rossendorf PET Centre in Dresden, Germany. Both studies were approved by a local research ethics board and were conducted in accordance with good clinical practice guidelines, all applicable regulatory requirements, and the Code of Ethics of the World Medical Association (Declaration of Helsinki). All subjects provided written informed consent. Both studies were completed before 2008 and are therefore not included in trial registries.

The radiolabeling methods for radiosyntheses at Dresden are given in the supplemental information (supplemental materials are available at http://jnm.snmjournals.org), and for Toronto the methods have been previously described (*8*).

Toronto Study

For this study, scans were obtained with an arterial input function to perform model-based kinetic analysis of ^{11}C-GSK215083 brain uptake. Seventeen healthy subjects (age, 33 ± 8 y; weight, 69 ± 15 kg [mean ± SD]; 8 men and 9 women) were enrolled in this single-session study to assess brain biodistribution of ^{11}C-GSK215083. Medical history, physical examination, electrocardiogram, and vital sign information were collected at screening and at follow-up (within 7 d of the scan).

On the study day, subjects were cannulated in the antecubital vein for tracer administration and in the contralateral radial artery for blood sampling. Subjects received a bolus intravenous injection of ^{11}C-GSK215083 (357 ± 15.34 MBq; mass dose, 3.25 ± 1.40 μg; maximum mass injected, 5.65 μg). After injection, dynamic data were acquired in list-mode using a Biograph HiRez XVI PET camera system (Siemens Molecular Imaging (*11*)). A low-dose CT transmission scan was obtained for attenuation correction.

For all scans, list-mode data were converted into a sequence of 26 frames (8 × 15 s, 3 × 1 min, 5 × 2 min, 5 × 5 min, and 5 × 10 min) for a total of 90 min. For each 3-dimensional sinogram, data were normalized and attenuation- and scatter-corrected before Fourier rebinning and conversion into 2-dimensional sinograms. Images were reconstructed using a 2-dimensional filtered backprojection algorithm, with a ramp filter at the Nyquist cutoff frequency. A gaussian filter of 5 mm in full width at half maximum was applied and images calibrated to Bq/cm^3. Images were combined to create a single dynamic dataset on which regions of interest (ROIs) were described and time–activity curves derived.

During acquisition, arterial blood samples were collected for the determination of whole-blood and -plasma input functions. The fraction of radioactivity in the plasma corresponding to authentic radioligand was determined by radio–high-performance liquid chromatography from 9 discrete arterial blood samples (between 2.5 and 75 min). The metabolite analysis method is described in the supplemental information.

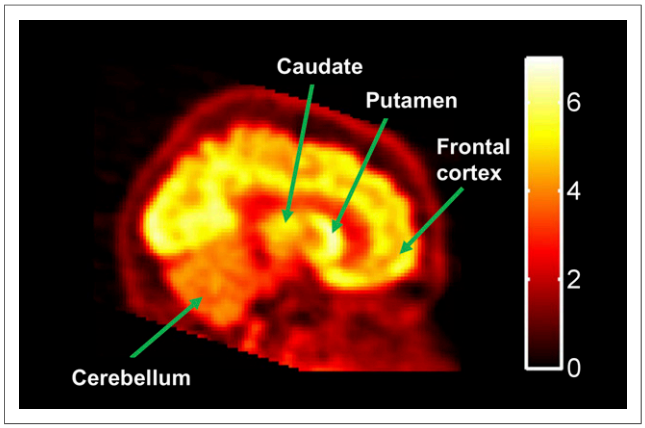

FIGURE 2. Baseline PET image demonstrating heterogeneous biodistribution of ^{11}C-GSK215083 in human brain (scale bar = percentage injected dose per liter).

TABLE 1
Regional Estimates of V_T from Models with Plasma Parent Input Functions

Region	4k (n = 14)	MA2 (n = 17)
Caudate	18.0 ± 11.2	12.14 ± 5.62
Putamen	17.2 ± 8.82	13.34 ± 6.20
Frontal cortex	9.28 ± 3.78	7.50 ± 2.17
Hippocampus	6.69 ± 2.04	5.84 ± 1.61
Cerebellum	6.12 ± 2.72	5.04 ± 1.45

Data are mean ± SD.

Dresden Study

This study was performed for pharmacologic characterization of ^{11}C-GSK215083 brain uptake, along with characterization of the receptor occupancy achieved on repeated dosing with SB742457. Eighteen healthy male subjects (age, 57 ± 4 y; weight, 81 ± 10 kg) were recruited into this open-label, adaptive study (AZ3103943). Three groups were enrolled. Group 1 (n = 4) assessed the test–retest reliability for each subject of 2 independent administrations of ^{11}C-GSK215083, 4–7 d apart (Fig. 1A).

Group 2 (n = 6) was used for pharmacologic characterization of the regional binding of ^{11}C-GSK215083. In addition to its affinity for 5HT6 receptors, the PET ligand ^{11}C-GSK215083 also possesses an approximately 5-fold-lower affinity for the 5HT2A receptor (*3*). Therefore, we used ketanserin, a selective 5HT2A antagonist, to test for the existence of detectable binding to 5HT2A receptors and SB742457 to detect binding to 5HT6 receptors. Four subjects underwent a baseline ^{11}C-GSK215083 scan followed by 2 further PET scans, after SB742457 (175 mg, orally, 5 h before ^{11}C-GSK215083 administration) and after ketanserin (0.1 mg/kg, by slow intravenous injection, 2 h before ^{11}C-GSK215083 administration), respectively, in a randomized fashion, 7 d apart. The remaining 2 subjects received a baseline scan, a second scan after SB742457 (175 mg), and a third scan, 7 d later (Fig. 1B).

Group 3 (n = 8) characterized the time and dose occupancy relationship of SB742457 in the brain. Each subject underwent 3 PET scans. Scan 1 was a baseline scan with scans 2 and 3 following repeated once-daily dosing of SB742457 on 2 occasions between 7 and 28 d of dosing. Four subjects received a loading dose of SB742457 (175 mg) on day 1, followed by 35 mg daily for 21 or 28 d (2 subjects per group). Subjects were randomized to undergo 2 scans on days 7, 14, 21, and 28, such that 2 independent data points were collected for each time point (Fig. 1C). Similarly, 2 further subjects received SB742457 (70 mg) followed by 15 mg daily for 14 d, and the last 2 subjects received 15 mg followed by 3 mg daily for 14 d. All 4 subjects were scanned on days 7 and 14 (Fig. 1D). Scans were conducted approximately 5 h after SB742457 dosing.

Safety assessments included medical history, physical examination, adverse event reporting, clinical laboratory assessments and electrocardiogram, blood pressure, and pulse rate measurements (supplemental information). Blood samples were collected for pharmacokinetic analysis of SB742457 in plasma from subjects in groups 2 and 3 before and on completion of each scan for which SB742457 was administered (supplemental information).

For each subject, a low-dose CT transmission scan was obtained for attenuation correction. Dynamic data were acquired in list-mode using an ECAT EXACT HR$^+$ PET camera system (Siemens Molecular Imaging). Recording of emission data began on bolus intravenous injection of ^{11}C-GSK215083 (338 ± 37 MBq; mass dose, 6.04 ± 1.61 μg; maximum mass injected, 10.36 μg). For all scans, list-mode data were converted into a sequence of 26 frames (8 × 15 s, 3 × 1 min, 5 × 2 min, 5 × 5 min, and 5 × 10 min), for a total of 90 min. Normalization and data reconstruction were conducted as in the Toronto study. Images were combined to create a single dynamic dataset on which ROIs were described and time–activity curves derived.

MR Images

In both studies, a T1-weighted anatomic 3-dimensional MR image was obtained for each subject (1.5-T Signa-Excite HD; GE Healthcare) for coregistration with the PET data and identification of discrete regional volumes (resolution, 1 × 1 × 1 mm).

Data Processing and Kinetic Analysis

Dynamic PET data were corrected for motion via frame-to-frame image registration and aligned with the structural T1-MR image using SPM5 (Wellcome Trust Centre for Neuroimaging) with a normalized mutual-information cost function.

ROIs (caudate, putamen, cortical regions, hippocampus, and cerebellum) were defined on the MR image for each subject using a region template (*12*). MR images were coregistered to the corresponding summed PET image and ROIs applied to the dynamic PET images to generate tissue time–activity curves. Of the cortical regions

Table 2
Regional BP Values for Different Kinetic Models

	Plasma input functions (BPs)		Reference tissue methods (BPs)		Akaike	
Brain region	4k	MA2	FRTM	SRTM	FRTM	SRTM
Caudate	1.787 ± 0.075	1.349 ± 0.621	1.767 ± 0.805	2.586 ± 1.910	91.166 ± 14.995	90.712 ± 13.272
Putamen	1.819 ± 0.758	1.587 ± 0.658	1.888 ± 0.954	2.450 ± 1.412	89.154 ± 17.230	88.295 ± 13.055
Hippocampus	0.074 ± 0.145	0.164 ± 0.072	0.180 ± 0.063	0.184 ± 0.066	79.521 ± 11.391	78.465 ± 11.439
Frontal lobe	0.522 ± 0.223	0.489 ± 0.102	0.473 ± 0.090	0.475 ± 0.091	47.517 ± 23.088	46.215 ± 20.646
Parietal lobe	0.569 ± 0.357	0.496 ± 0.089	0.478 ± 0.077	0.481 ± 0.077	47.296 ± 23.963	43.441 ± 22.293
Occipital lobe	0.383 ± 0.564	0.524 ± 0.084	0.496 ± 0.061	0.500 ± 0.059	51.289 ± 22.605	46.615 ± 20.627
Temporal lobe	0.335 ± 0.594	0.484 ± 0.102	0.464 ± 0.089	0.468 ± 0.094	51.756 ± 16.586	50.292 ± 16.778

Data are mean ± SD.

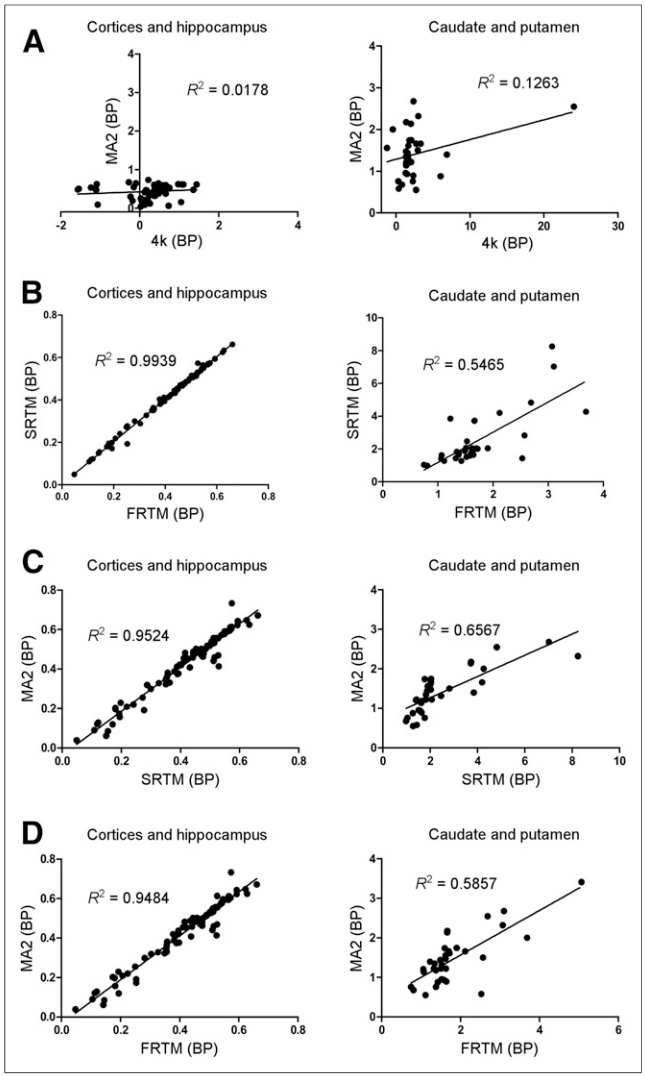

FIGURE 3. Correlations between estimates of BP_{ND} obtained from 4 kinetic models across striatal, hippocampal, and cortical regions. (A) 4k vs. MA2. (B) FRTM vs. SRTM. (C) SRTM vs. MA2. (D) FRTM vs. MA2.

(frontal, parietal, occipital, and temporal), analytic results were similar within each subject, and subsequently only those for the frontal cortex are presented.

Toronto Data Analysis. Data from the 17 subjects were fitted initially to 4 separate arterial plasma input models: 3 compartmental models and the multilinear model MA2 (*13*), each containing a parameter to account for dispersion of blood in the withdrawal cannula (*14*).

Models fitted included a 1-tissue-compartment model with clearance and rate constants K_1 and k_2, between plasma and tissue (2k); a 2-tissue-compartment model, with 1-reversible-tissue compartment feeding a second irreversible tissue compartment with rate constant k_3 (3k); a 2-reversible-tissue-compartment model with exchange rate constants k_3 and k_4 (4k); and the multilinear model MA2, applicable to reversible radioligands (*13*) and involving linear transforms of the plasma and tissue data based on a reversible 4k model. Fits of the data to these models were compared on the basis of an Akaike information criterion (*15*), with individual data points weighted by frame length. In addition, data were also analyzed using a simplified reference tissue model (SRTM) and full reference tissue model (FRTM) using the cerebellum as the reference region (*16*).

Dresden Data Analysis. Metabolite-corrected arterial plasma input functions were not available, and hence data were analyzed using the SRTM and FRTM models.

RESULTS

Kinetic Modeling of 5HT6 PET Radioligand ^{11}C-GSK215083

A representative baseline image for ^{11}C-GSK215083 uptake is given in Figure 2, where ^{11}C-GSK215083 readily enters the brain with the highest uptake observed in the caudate and putamen (striatum), moderate levels in the cortex, and lowest uptake in the cerebellum.

Data from the Toronto subjects were analyzed using the 3 compartmental models along with the multilinear model MA2. Model 2k was the least favorable of these 3 models in all regions for all subjects. For 10 subjects, the 4k model performed better than the 3k model. However, the relatively slow kinetics of this radioligand were associated with model 3k performing better in all or most regions of the remaining 7 subjects.

For 3 of the 7 subjects that best fitted the 3k model, large estimates of volume of distribution (V_T) were obtained in some/all regions when the 4k model was applied to these datasets. However, there was no consistent distribution of best-fit models between the high-binding striatal regions and other regions with relatively lower levels of binding. When the MA2 model was applied to the ROI data, there were no apparent outliers in the estimates of V_T across all regions for the 17 subjects, as determined via visual inspection. Estimates of the regional V_T are given in Table 1, for both the 4k and the MA2 models (excluding outliers for model 4k), where estimates from the 4k model were consistently higher than the MA2 model.

Regional values for the BP for the nondisplaceable component (BP_{ND}) were subsequently calculated from the estimates of V_T obtained from the 4k and MA2 models, assuming the cerebellum was a suitable reference region (Table 2). In addition, the binding potential for the BP_{ND} was also estimated from the regional time–activity curve using the FRTM and the SRTM with the cerebellum acting as the reference region. These models were applied to all 17 subjects, and the results are given in Table 2. Of the 2 reference region models, FRTM showed less intersubject variability in the high-binding striatal regions than SRTM. Although there was a close agreement in the estimates between the 2 reference tissue models and model MA2 in regions with low and intermediate binding regions (e.g., hippocampus and cortex), there was more variation observed between models in the high-binding striatal regions.

Correlations between the estimates of BP_{ND} obtained from the 4 models across the striatal, hippocampal, and cortical regions are given in Figure 3.

Collectively, these data suggest that the MA2 model can be used as a preferred method for analyzing human ^{11}C-GSK215083 PET data when a blood input is available and the FRTM method as a suitable alternative in the absence of any arterial input function.

^{11}C-GSK215083 Test–Retest

Test–retest data from the 4 subjects scanned at Dresden are given in the supplemental information.

^{11}C-GSK215083 Pharmacologic Characterization

The effects of the 5HT2A antagonist ketanserin and the dual 5HT6/5HT2A antagonist SB742457 on ^{11}C-GSK215083 BP_{ND} in the brain at 5 h after administration are given in Table 3. The caudate and putamen both represent 5HT6 densely populated

structures whereas the frontal cortex represents a 5HTA-rich region. SB742457 occupied 64% and 84% of the putamen and caudate signal, respectively, and 63% of the frontal cortical signal.

Ketanserin occupied 25% of the frontal cortical signal at 5 h after administration and only 3% and 16% of the putamen and caudate signal, respectively. Interestingly, high occupancies in both the putamen and the caudate were observed (range, 70%–86%) after ketanserin administration in the 2 subjects (6 and 7) who received SB742457 followed by ketanserin 7 d later. To determine whether these high occupancies were due to ketanserin itself or a potential carryover of SB742457 from the previous scan 7 d earlier, 2 further subjects were studied who received SB742457 and were scanned 5 h and 7 d after administration (subjects 9 and 10; Table 3). Data from these 2 subjects demonstrated occupancies of 57% (5 h) and 56% (7 d) in the putamen and 91% (5 h) and 87% (7 d) in the caudate. These findings strongly suggest the ketanserin data for subjects 6 and 7 would have been compromised from SB742457 being administered 7 d earlier, and that SB742457 is present in the central nervous system for longer than 7 d.

^{11}C-GSK215083 Dose Occupancy

The effect of repeated SB742457 administration on ^{11}C-GSK215083 uptake into the human brain was assessed at 3 dose levels, given in Table 4 and Figure 4. Repeated exposure of 3, 15, and 35 mg/d exhibited near-to-complete occupancy of the 5HT6-containing regions (putamen and caudate) and a dose-dependent increase in occupancy in the frontal cortex.

Correlation of Plasma Pharmacokinetic and PET Pharmacokinetic Data

Plasma pharmacokinetic data after acute administration of SB742457 (175 mg) in humans is given in Figure 5A. These pharmacokinetic data demonstrate the mean concentration of SB742457 to be approximately 30 ng/mL at 96 h after administration. A subsequent correlation of plasma pharmacokinetic data together with the PET pharmacokinetic data for the frontal cortex region after repeated dosing of SB742457 (Fig. 5B) showed a clear dose occupancy curve exhibiting a median effective dose of 92.38 ng/mL of SB742457 in the plasma.

TABLE 3
Effect of Ketanserin and SB742457 on ^{11}C-GSK215083 BP_{ND} in Putamen, Caudate, and Frontal Cortex at 5 Hours and 7 Days After Administration

	FRTM BP, ketanserin			FRTM BP, SB-742457		% occupancy	
Subject no.	Baseline	5 h	% occupancy, 5 h	5 h	Day 7	5 h	Day 7
Putamen (5HT6)							
Subject 5	0.865	0.882	0	0.419	~	52	~
Subject 6*	1.196	0.359	70	0.292	~	76	~
Subject 7*	1.466	0.306	79	0.378	~	74	~
Subject 8	1.449	1.355	6	0.437	~	70	~
Subject 9	1.020	~	~	0.407	0.376	60	63
Subject 10	0.837	~	~	0.387	0.430	54	49
Mean			3			64	56
Caudate (5HT6)							
Subject 5	0.655	0.594	9	0.226	~	65	~
Subject 6*	0.768	0.190	75	0.160	~	79	~
Subject 7*	0.546	0.075	86	0.098	~	82	~
Subject 8	1.839	1.413	23	0.114	~	94	~
Subject 9	0.955	~	~	0.163	0.198	83	79
Subject 10	0.713	~	~	0.005	0.045	99	94
Mean			16			84	87
Frontal cortex (5HT2A)							
Subject 5	0.212	0.185	13	0.052	~	75	~
Subject 6*	0.272	Poor fit	~	0.050	~	81	~
Subject 7*	0.390	0.281	28	0.175	~	55	~
Subject 8	0.277	0.178	36	0.145	~	48	~
Subject 9	0.202	~	~	0.059	0.136	71	33
Subject 10	0.326	~	~	0.163	0.249	50	24
Mean			25			63	29

*Subjects who received SB742457 before ketanserin.

TABLE 4
Effect of Repeated SB742457 Administration on ^{11}C-GSK215083 Uptake into Putamen, Caudate, and Frontal Cortex at 3 Dose Levels

	FRTM BP					% occupancy				
Subject no.	Baseline	Day 7	Day 14	Day 21	Day 28	Day 7	Day 14	Day 21	Day 28	Mean occupancy
Putamen (5HT6)										
Subject 11	1.085	No scan	~	0.346	~	No scan	~	68	~	68
Subject 12	0.909	0.324	~	~	0.297	64	~	~	67	66
Subject 13	1.001	~	0.283	0.300	~	~	72	70	~	71
Subject 14	1.359	~	0.300	~	0.328	~	78	~	76	77
										70
Subject 15	0.994	0.307	0.397	~	~	69	60	~	~	65
Subject 16	1.042	0.295	0.312	~	~	72	70	~	~	71
										68
Subject 17	0.890	0.350	0.411	~	~	61	54	~	~	58
Subject 18	1.052	0.379	0.328	~	~	64	69	~	~	67
										62
Caudate (5HT6)										
Subject 11	0.510	No scan	~	0.037	~	No scan	~	93	~	93
Subject 12	0.912	0.067	~	~	0.178	93	~	~	81	87
Subject 13	1.092	~	0.051	0.173	~	~	95	84	~	90
Subject 14	1.044	~	0.010	~	0.121*	~	99	~	88*	99
										92
Subject 15	0.754	Poor fit	0.336	~	~	Poor fit	55	~	~	55
Subject 16	0.697	−0.052	0.004	~	~	108	99	~	~	104
										79
Subject 17	0.944	0.051	0.009	~	~	95	99	~	~	97
Subject 18	1.746	−0.061181	−0.027	~	~	104	102	~	~	103
										100
Frontal cortex (5HT2A)										
Subject 11	0.272	No scan	~	0.191	~	No scan	~	30	~	30
Subject 12	0.228	0.087	~	~	0.108	62	~	~	53	58
Subject 13	0.238	~	0.048	0.080	~	~	80	67	~	74
Subject 14	0.257	~	0.096	~	0.072	~	63	~	72	68
										57
Subject 15	0.373	0.277	0.196	~	~	26	48	~	~	37
Subject 16	0.273	0.162	0.211	~	~	41	23	~	~	32
										35
Subject 17	0.280	0.190	0.213	~	~	32	24	~	~	28
Subject 18	0.269	0.223	0.215	~	~	17	20			19
										23

*SRTM value (FRTM value = 0.48808).

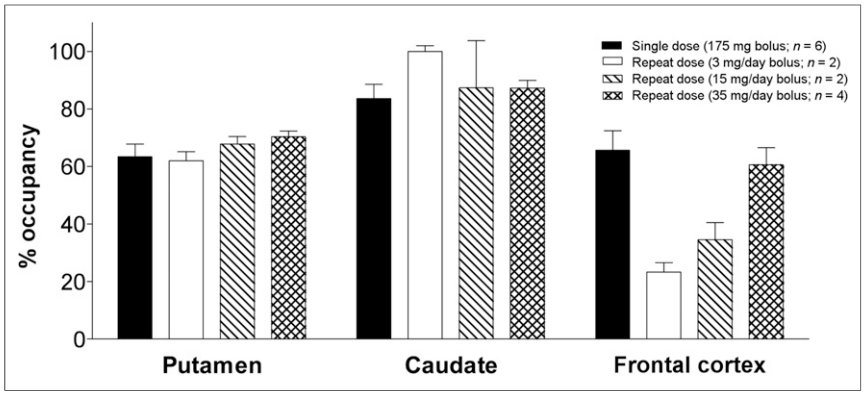

FIGURE 4. Graph demonstrating dose-dependent increase in occupancy of 5HT2A receptor after increasing doses of SB742457 in frontal cortex and near-to-complete occupancy of 5HT6 receptor at all doses administered (FRTM analysis).

DISCUSSION

This article reports kinetic modeling of the 5HT6 PET radioligand ^{11}C-GSK215083 in the human brain using both plasma input and reference tissue quantification approaches; pharmacologic characterization of ^{11}C-GSK215083 in the brain using the pharmacologic tools ketanserin (5HT2A-selective) and SB742457 (5HT6/5HT2A-selective); and 5HT6 and 5HT2A occupancies achieved on repeated dosing with SB742457.

Of the kinetic models that required the use of an arterial input function, the MA2 model represented the method of choice for analyzing human ^{11}C-GSK215083 PET data, with all datasets able to fit to this model (Tables 1 and 2), consistent with the notion that ^{11}C-GSK215083 represents a reversible radioligand with slow kinetics in high-binding regions. Of the reference tissue models, the FRTM demonstrated slightly lower intersubject variability than the SRTM (Table 2). Collectively, these data indicate that the MA2 model could be used for the analysis of human ^{11}C-GSK215083 PET data when a blood input is available, and in the absence of a blood input the FRTM represents a suitable alternative.

In addition to its affinity for 5HT6 receptors, the PET ligand GSK215083 also possesses an approximately 5-fold-lower affinity for the 5HT2A receptor (*3*). 5HT2A receptors are known to exist in high densities in the cortex, with moderate-to-negligible levels in the striatum and low levels in the cerebellum (*17*). Subsequently, colocalization of 5HT6 and 5HT2A receptors in particular areas of the brain require the use of selective compounds to delineate the uptake of ^{11}C-GSK215083 associated with each of these target proteins.

After acute dosing with the 5HT2A receptor antagonist ketanserin, occupancies of approximately 25% in the frontal cortical region and 3%–16% in the striatal regions were observed. In addition, acute administration of the dual 5HT6/5HT2A antagonist SB742457 demonstrated occupancies of approximately 63% in the frontal cortex and 64%–84% in the striatal regions (Table 3).

The apparent lack of occupancy in the striatal regions after ketanserin and the high occupancy after SB742457 administration suggest this brain region to be mainly 5HT6-containing. In contrast, the cortex is known to contain a much higher density of 5HT2A receptors than 5HT6 receptors. The high level of occupancy in the cortical region by SB742457 almost certainly points toward blockade of the 5HT2A receptor, thereby reflecting the dual action of this compound on both 5HT6 (striatal region) and 5HT2A receptors (frontal cortex).

The unexpected discovery of a single dose of SB742457 (175 mg) producing prolonged occupancy at the striatal 5HT6 receptors for a period of at least 7 d was revealed after randomization of dosing for ketanserin and SB742457 in the same subjects. Human plasma pharmacokinetic data for this compound demonstrated a mean concentration of SB742457 (175 mg) to be approximately 30 ng/mL at 4 d after administration, and hence negligible levels were expected to be present at 7 d after administration (Fig. 5A). Consequently, for SB742457 the plasma pharmacokinetic data were not reflected by the tissue occupancy data measured at 7 d after administration, and this is most probably due to the subnanomolar affinity of this compound for the 5HT6 receptor in the striatal tissue (0.25 nM (*6*)).

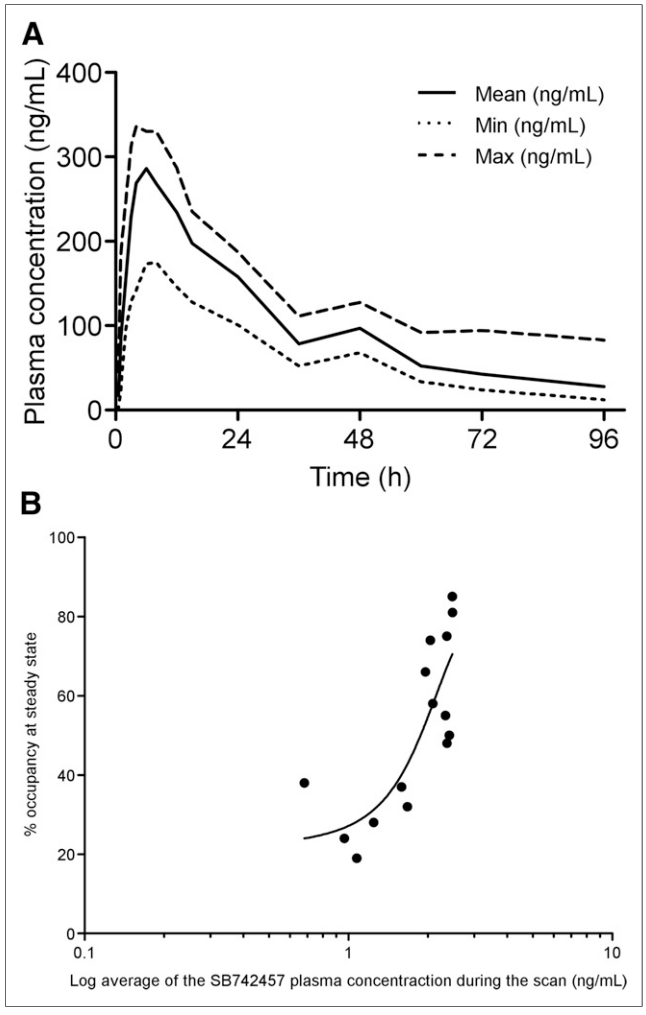

FIGURE 5. Pharmacokinetic data for SB742457. (A) Human plasma pharmacokinetic data for SB742457. (B) Correlation of plasma pharmacokinetic data vs. percentage 5HT2A PET receptor occupancy (FRTM) at different doses of SB742457. max = maximum; min = minimum.

Repeated dosing of SB742457 in healthy subjects demonstrated a dose-dependent increase in occupancy of the 5HT2A receptors in the frontal cortex while maintaining a near-to-complete occupancy in the striatal regions at all dose levels administered (Table 4; Fig. 4). The approximately 40-fold-lower affinity of SB742457 for the 5HT2A (inhibitory constant, 10 nM (*6*)) than the 5HT6 receptor (inhibitory constant, 0.25 nM) may account for this dose occupancy effect observed for the 5HT2A receptors in the cortex.

Chronic dosing of SB742457 to subjects with mild-to-moderate AD has previously demonstrated a statistically significant improvement in the CIBIC+ scale over a 24-wk period (*5*). In this study, 3 dose levels were investigated (5, 15, and 35 mg once daily for 24 wk) in a randomized, double-blind, placebo-controlled study in 357 subjects with mild-to-moderate probable AD. The highest dose level (35 mg) separated from placebo on the CIBIC+ score, whereas the lower doses did not. The current PET study indicates that the pharmacologic differences between the 3 doses were not related to various degree of occupancy of 5HT6 receptors (which appeared to be saturated at these 3 dose regimens), rather the difference between low and high doses was the progressive involvement of 5HT2A receptors. These data suggest that antagonism at both receptors is required for therapeutic effects of SB742457.

Antagonism of the human 5HT2A and D2 receptors in patients with schizophrenia via the commonly used antipsychotic risperidone has previously demonstrated positive effects on working memory, executive functioning, and attention, whereas improvement in verbal learning and memory have been more inconsistent (*18*). In a recent study by Rainer et al. (*19*), 34 patients with a DSM-IV diagnosis of dementia (Alzheimer type, vascular, mixed or with Lewy bodies) were treated with flexible doses of risperidone (0.5–2 mg/d) for 8 wk, and at the end of treatment improvements in symptoms (clinical global impression of change scale) were reported for 82% of patients and additionally cognitive function was maintained throughout the treatment period.

Studies reported in the literature indicate that SB742457 enhances cognitive performance in patients with mild-to-moderate AD (*5,6*), which is purported to be via antagonism of the 5HT6 receptor. Because SB742457 also demonstrates a high affinity for the 5HT2A receptor (albeit ~40-fold lower than the 5HT6), it must be considered whether antagonism of this receptor may also play a role in enhancing the cognitive-enhancing properties of SB742457. Current clinical literature does not support cognitive-enhancing effects of SB742457 via antagonism of the 5HT2A receptor alone; however, the effect of antagonizing both the 5HT6 and the 5HT2A simultaneously should be considered as a possible mechanism of action for SB742457.

To fully elucidate the mechanism of action for the cognitive-enhancing properties of SB742457, further studies will be required that combine both imaging methods and efficacy assessments of cognitive performance (e.g., Alzheimer's Disease Assessment Scale Cog and CIBIC+) to correlate clinical benefit with receptor occupancy for potential therapeutic benefit of this compound in AD.

CONCLUSION

This article reports full kinetic modeling of the 5HT6 PET radioligand ^{11}C-GSK215083 in the human brain, where the multilinear model MA2 represents the method of choice for analyzing ^{11}C-GSK215083 PET data when a blood input is available and the FRTM when a blood input is not available. Pharmacologic evaluation suggests that ^{11}C-GSK215083 binds to the 5HT6 in the striatum and to the 5HT2A in the cortex. Furthermore, the data suggest that for SB742457, a regimen of 35 mg/d would be associated with antagonism at both receptors, whereas lower doses of 5 and 15 mg/d would block only the 5HT6 receptors. These data suggest that engagement of both 5HT2A and 5HT6 receptors might be desirable to achieve superior efficacy of SB742457 in AD.

DISCLOSURE

The costs of publication of this article were defrayed in part by the payment of page charges. Therefore, and solely to indicate this fact, this article is hereby marked "advertisement" in accordance with 18 USC section 1734. At the time this work was conducted Christine A. Parker, Eugenii A. Rabiner, Roger N. Gunn, Graham Searle, Laurent Martarello, Robert A. Comley, Marc Laruelle, Maria Davy, and Vincent J. Cunningham were employees of and owners of stock/options in GlaxoSmithKline. Alan A. Wilson and Sylvain Houle have received grants from GlaxoSmithKline. No other potential conflict of interest relevant to this article was reported.

ACKNOWLEDGMENTS

We thank staff at the CAMH PET Centre (particularly Irina Vitcu, Alvina Ng, Peter Bloomfield, Jeannie Fong, Armando Garcia, Winston Stableford, and Min Wong) and staff at the Radiologische Gemeinschaftspraxis MRI Centre, ABX-CRO, and Forschungszentrum Rossendorf PET facility, Dresden, Germany (particularly Martin Siepmann, Andreas Kluge, Frank Wurst, and Joerg van den Hoff), for technical assistance and performance of the clinical studies. Additionally, we thank members of the GSK CIC, Clinical Pharmacokinetics (particularly Bart Laurijssens), CSSO, and medicinal chemistry teams for their support. The GlaxoSmithKline-sponsored clinical studies at both CAMH and Dresden were investigator-led and performed on behalf of GlaxoSmithKline.

REFERENCES

1. Woolley ML, Marsden CA, Fone KCF. 5-ht6 receptors. *Curr Drug Targets CNS Neurol Disord.* 2004;3:59–79.
2. Hirst WD, Abrahamsen B, Blaney FE, et al. Differences in the central nervous system distribution and pharmacology of the mouse 5-hydroxytryptamine-6 receptor compared with rat and human receptors investigated by radioligand binding, site-directed mutagenesis, and molecular modelling. *Mol Pharmacol.* 2003;64:1295–1308.
3. Parker CA, Gunn RN, Rabiner EA, et al. Radiosynthesis and characterization of ^{11}C-GSK215083 as a PET radioligand for the 5-HT6 receptor. *J Nucl Med.* 2012;53:295–303.
4. Chuang AT, Foley A, Pugh PL, et al. 5-HT6 receptor antagonist SB-742457 as a novel cognitive-enhancing agent for Alzheimer's disease. *Alzheimers Dement.* 2006;2(suppl):S631–S632.
5. Maher-Edwards G, Zvartau-Hind M, Hunter AJ, et al. Double-blind, controlled phase II study of a 5-HT6 receptor antagonist, SB-742457, in Alzheimer's disease. *Curr Alzheimer Res.* 2010;7:374–385.
6. Maher-Edwards G, Dixon R, Hunter J, et al. SB-742457 and donepezil in Alzheimer disease: a randomized, placebo-controlled study. *Int J Geriatr Psychiatry.* 2011;26:536–544.

7. Liem-Moolenaar M, Rad M, Zamuner S, et al. Central nervous system effects of the interaction between risperidone (single dose) and the 5-HT6 antagonist SB742457 (repeated-doses) in healthy men. *Br J Clin Pharmacol.* 2011;71: 907–916.
8. Comley RA, Salinas C, Mizrahi R, et al. Biodistribution and radiation dosimetry of the serotonin 5-HT6 ligand [^{11}C]GSK215083 determined from whole body PET. *Mol Imaging Biol.* 2012;14:517–521.
9. Ahmed M, Johnson CN, Jones M, et al., inventors; Glaxo Group Limited, assignee. Quinoline derivatives and their use as 5-HT6 ligands. International patent application PCT/EP3003/003197. March 25, 2003.
10. Gee AD, Martarello L, Johnson CN, Witty DR, inventors; Glaxo Group Limited, assignee. Radiolabelled quinoline-based ligands for the 5-HT6 receptor functionality. International patent application PCT/EP2005/012463. November 17, 2005.
11. Brambilla M, Secco C, Dominietto M, Matheoud R, Sacchetti G, Ingelese E. Performance characteristics obtained for a new 3-dimensional lutetium oxyorthosilicate-based whole-body PET/CT scanner with the National Electrical Manufacturers Association NU 2-2001 standard. *J Nucl Med.* 2005;46:2083–2091.
12. Hammers A, Koepp MJ, Free SL, et al. Implementation and application of a brain template for multiple volumes of interest. *Hum Brain Mapp.* 2002;15: 165–174.
13. Ichise M, Toyama H, Innis RB, Carson RE. Strategies to improve neuroreceptor parameter estimation by linear regression analysis. *J Cereb Blood Flow Metab.* 2002;22:1271–1281.
14. Ashworth S, Rabiner EA, Gunn RN, et al. Evaluation of ^{11}C-GSK189254 as a novel radioligand for the H3 receptor in humans using PET. *J Nucl Med.* 2010;51:1021–1029.
15. Akaike H. A new look at the statistical model identification. *IEEE Trans Automat Contr.* 1974;19:716–723.
16. Gunn RN, Lammertsma AA, Hume SP, et al. Parametric imaging of ligand-receptor binding in PET using a simplified reference region model. *Neuroimage.* 1997;6:279–287.
17. Forutan F, Estalji S, Beu M, et al. Distribution of 5HT2A receptors in the human brain: comparison of data in vivo and post mortem. *Nuklearmedizin.* 2002;41: 197–201.
18. Meltzer HY, McGurk SR. The effects of clozapine, risperidone, and olanzapine on cognitive function in schizophrenia. *Schizophr Bull.* 1999;25:233–255.
19. Rainer MK, Masching AJ, Ertl MG, et al. Effect of risperidone on behavioral and psychological symptoms and cognitive function in dementia. *J Clin Psychiatry.* 2001;62:894–900.